SIAM J. APPL. MATH.
Vol. 60, No. 4, pp. 1425–1446

BIOCHEMICAL REACTIONS ON HELICAL STRUCTURES*

D. A. EDWARDS†

Abstract. Analyses of biochemical surface-volume reactions often focus on the reaction-dominated case, where the free-floating analyte is well-mixed and the binding kinetics are unaffected by transport. In actuality, transport effects often play a role. A mathematical model is formulated for a cylinder with a helical reacting strip on its surface, which is a good model for a helical biopolymer such as DNA that interacts with molecules that bind to periodic structures along its backbone. Perturbation techniques are used to analyze the concentration of the reacting species for association and dissociation kinetics when the cylinder is immersed in a quiescent medium. In the case of an insulating boundary for the analyte region, a multiple-scale expansion must be used. The secularity which necessitates such an expansion is significantly different from canonical examples. The expressions for the bound state provide a direct way to estimate the rate constants from raw data. Remarks on the calculation of effective rate constants for general transport-affected systems are presented.

Key words. perturbation methods, ligand-receptor kinetics, transport-influenced kinetics, surface-volume reactions, DNA, multiple-scale methods

AMS subject classifications. 35B25, 35C20, 35K60, 76R99, 80A30, 92C45

PII. S0036139998343769

1. Introduction.

The study of biochemical reactions is of great importance to the biological sciences. Many chemical reactions of interest in biological systems are two-component reactions where one of the reactants is confined to a surface (often receptors on a cell membrane), while the other is immersed in a volume. For instance, receptors confined to the surface of a cell react with ligands floating in the cytoplasm [1]. In addition, gene expression is significantly influenced by DNA-protein interactions in these geometries [2]. Cylindrical geometries are of particular interest due to their relationship to DNA structures [3] and certain rod-shaped viruses, such as the tobacco mosaic virus [4].

To understand such reactions better, scientists need accurate estimates of the association rate constant $\tilde{k}_{\mathrm{a}}$ and the dissociation rate constant $\tilde{k}_{\mathrm{d}}$. Clearly the full mathematical model for such a system must include not only the biochemical reaction, but also the transport of the free-floating reactant (the *analyte*) to the reacting surface.

Certainly there have been many studies of systems where transport and reactions occur (for instance, see the standard textbook [5]). More novel is the study of transport effects where the reaction occurs on a surface. Such systems occur in chemical vapor deposition (CVD) processes when one is trying to produce a reaction on a thin film. However, the reactants in these systems are in gaseous form rather than dissolved in a liquid [6], [7], [8], [9]. In fixed-bed reactors, gaseous components diffuse through highly porous catalysts to react on "active sites." However, the dynamics of the surface reaction are highly complicated and hence not well known [10].

Rusu [11] treats the case of a reaction that occurs on the inside of a closed tube down which a reactant flows. Rusu expands upon previous work in [12], [13] which treats only first-order reactions. Clearly this particular geometry is a good model for

*Received by the editors August 19, 1998; accepted for publication (in revised form) April 12, 1999; published electronically April 20, 2000.
http://www.siam.org/journals/siap/60-4/34376.html
†Department of Mathematical Sciences, University of Delaware, Newark, DE 19716-2553 (edwards@math.udel.edu).

clot formation in blood flow [12], [13], [14], [15], [16], but the solutions will be quite different from those for the geometry outside a cylinder which we shall consider here. Not all authors use a reaction model; some use an integral adhesion approach [16].

Many authors decouple the reaction kinetics from the transport dynamics [9], [14]. When one does so, the equations that result are easily solved in terms of exponentials [17]. Unfortunately, this decoupling occurs only when the parameter values are in certain ranges [18], [19], which happens when the reaction and transport occur on disparate time scales.

If the parameters do not fall in these ranges, transport effects must be included in the analysis [15]. There have been some numerical simulations [20] and modeling [21] of all the dynamics in similar systems, but few analytical studies have been undertaken [11], [19], [22], [23]. Rather than modeling the full transport-reaction system, some authors prefer to introduce a new "mass transfer coefficient" to account for diffusive effects [18], [24]. Through a careful analysis, the expressions for these mass transfer coefficients may be directly derived from the full system of equations [23].

In this work we analyze a system in which a helical strip on a cylindrical surface contains the receptors, which mirrors the structure of the phosphate backbone of a DNA strand [3], [4]. The cylinder is immersed in a quiescent medium, so the transport is solely due to diffusion. We utilize the *two-compartment model* [1], [22], [25], so the analyte is considered to be floating in a second cylinder enclosing the first. Through scaling arguments, we show that there are three distinct time scales: one each for diffusion in the bulk solution, diffusion into the binding surface, and reaction on the binding surface. The flow away from the cylinder equilibrates on the diffusive time scale, and then the bound concentration evolves on the longer of the remaining two time scales.

The key dimensionless group is the Damköhler number (Da), which measures the ratio of the time scales of reaction and transport. In the limit that $\mathrm{Da} \to 0$, the transport and kinetic effects decouple and the equations reduce to the well-known case. Using Da as a small parameter, we construct the first-order correction to the reaction-limited case caused by small transport effects. In the case of the Dirichlet condition on the outer surface of the second compartment, the analysis is relatively straightforward, and the correction due to transport may be estimated by summing the first several terms in a Fourier series.

However, in the case of a no-flux condition on the outer surface of the second compartment, the analysis becomes more complicated. If one analyzes the system only on the slow reaction time scale, one obtains Laplace's equation, insulated at one boundary with a nonzero flux at the other, which has no solution. If one analyzes the system only on the faster diffusion time scale, one finds a constant forcing from the reaction that yields divergent results. Therefore, a multiple-scale expansion that considers both time scales must be introduced. However, note that the secularity arises in a vastly different way from that in a standard multiple-scale problem. (A further discussion of this type of multiple-scale problem may be found in [26].) Once the multiple-scale expansion has been postulated, the correction due to transport may be calculated using a Fourier series.

Using these expressions, we may adapt the standard ODE for the equilibrium case to include the effects of transport. The new equation that results is asymptotic to the true solution to leading two orders. In addition, the ODE has coefficients that can easily be interpreted as effective rate constants, which show how transport effects perturb the interpretation of measured data. Motivated by this phenomenon, some

general remarks are presented to show how one may derive effective rate constants for a class of problems that occur widely in these systems.

2. Governing equations. We study the effects of transport on a chemical reaction that occurs on a portion of the surface of a cylindrical structure of radius $\tilde{r} = r_c$, such as DNA. Though other more complicated means of transport could be considered, we begin by examining the case of a stationary cylinder in a quiescent medium, so diffusion is the only transport mechanism. Thus, the entire medium can be considered to be in the *Lévêque regime* [14], also called the *unstirred layer*. This layer, where diffusion is the dominant means of transport, also occurs in CVD systems [9].

We note that often in biological systems, the analyte can have a diameter $2r_a$ (where the subscript "a" stands for analyte) which is comparable to or larger than r_c. A typical value of r_c for a DNA strand is 10^{-7} cm [3]. When binding to the minor groove of DNA, the drug berenil spans three base-pair sites [27]. Since these base pairs are 3.4×10^{-8} cm apart [28], we have an r_a value comparable to r_c. In addition, berenil also sports a right-handed twist of 9.6×10^{-8} cm [27], which again is comparable to r_c. The DNA groove binder distamycin-A (compound GDH060 in the NDB nucleic acid data base [29]) and its related compounds span four or five base pairs [30], [31]. Moreover, crystallographic data in the NDB yield a characteristic radius of up to 2.19×10^{-7} cm.

Thus, we see that if the center of an analyte molecule diffuses to within a distance r_a of r_c, we expect the reaction to occur if the kinetics are favorable. Thus, we can idealize the analyte molecule as a point if we introduce an *effective radius* $r_{\text{eff}} = r_a + r_c$ which in the mathematical formulation replaces $\tilde{r} = r_c$ as the surface on which the reaction occurs. Therefore, the transport equation should hold in a region where $\tilde{r} > r_{\text{eff}}$.

Due to the cylindrical nature of the diffusion problem, we would expect to encounter logarithmic singularities if we considered the problem of a single cylinder in an infinite medium. Therefore, we utilize the so-called *compartment model* [1], [22], [25]; that is, we assume that there is an outer cylinder of finite radius Rr_{eff} containing the analyte. Then by taking R large, we can obtain reasonable approximations to the behavior of the cylinder in an infinite medium.

However, in more realistic laboratory situations one encounters other arrangements in which the two-compartment model is also useful. For instance, one can consider the helix to be immobilized in a cell or cell nucleus. Alternatively, one can perform an experiment with a periodic array of cylinders. In this case, the space between two cylinders may be idealized as a compartment with reflecting boundary conditions determined from symmetry considerations [32], [33], [34]. Then the quantity $(r_c/Rr_{\text{eff}})^2$ would approximate the area fraction of DNA in the solution.

Given these assumptions, the dimensional equation of motion is as follows:

$$\frac{\partial \tilde{C}}{\partial \tilde{t}} = D\left[\frac{1}{\tilde{r}}\frac{\partial}{\partial \tilde{r}}\left(\tilde{r}\frac{\partial \tilde{C}}{\partial \tilde{r}}\right) + \frac{1}{\tilde{r}^2}\frac{\partial^2 \tilde{C}}{\partial \theta^2} + \frac{\partial^2 \tilde{C}}{\partial \tilde{z}^2}\right], \tag{2.1}$$
$$\tilde{r} \in [r_{\text{eff}}, Rr_{\text{eff}}], \quad \theta \in [0, 2\pi], \quad \tilde{z} \in [0, 2\pi L],$$

where $\tilde{C}$ is the concentration of the analyte in the medium, D is the molecular diffusion coefficient for the system, θ is the angular coordinate, and $\tilde{z}$ is distance along the cylinder. The interpretation of L will be discussed below.

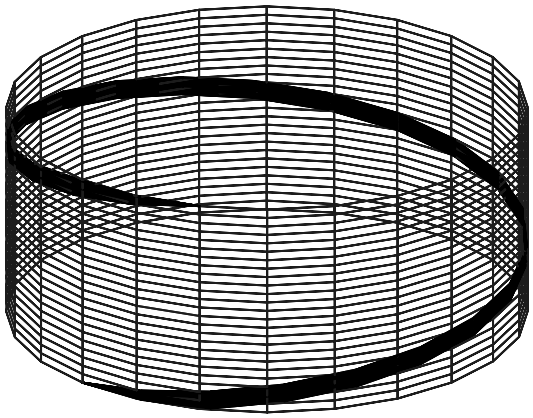

FIG. 2.1. *Cylinder with helical reacting strip.*

The initial analyte concentration is taken to be uniform:

$$\tilde{C}(\tilde{r},\theta,\tilde{z},0) = C_{\mathrm{T}}. \tag{2.2}$$

At the external radius $\tilde{r} = r_{\mathrm{eff}}R$, we have two possible boundary conditions. First, we can maintain a no-flux condition, which would correspond to a sealed experiment,

$$\frac{\partial \tilde{C}}{\partial \tilde{r}}(r_{\mathrm{eff}}R,\theta,\tilde{z},\tilde{t}) = 0, \tag{2.3a}$$

or we can maintain the analyte concentration at a fixed value, which we take to be equal to the initial condition,

$$\tilde{C}(r_{\mathrm{eff}}R,\theta,\tilde{t}) = C_{\mathrm{T}}. \tag{2.3b}$$

The last conditions to impose are at the binding surface. We consider the case where a binding protein in solution interacts with a site that is repeated periodically along a helical strip, such as the phosphate backbone or minor groove of DNA [3], [27]. We assume that this strip is of uniform width w (in radians), and that its endpoints vary linearly with $\tilde{z}$ (see Figure 2.1). This helix will then have a periodic structure in $\tilde{z}$. We denote the period by $2\pi L$, and hence we have that the reacting strip is the range

$$\frac{\tilde{z}}{L} \le \theta \le \frac{\tilde{z}}{L} + w. \tag{2.4}$$

Due to the periodicity of the helical structure, the cylinder is $2\pi L$-periodic in the $\tilde{z}$-direction. We note that with only one reacting strip, the model is closer to a segment of an α-helix than DNA. However, the consideration of two reacting strips is a simple extension of the analysis below.

The flux into the reacting strip is equal to the rate of change of the bound receptor concentration, which we denote by $\tilde{B}(\theta,\tilde{z},\tilde{t})$:

$$D\frac{\partial \tilde{C}}{\partial \tilde{r}}(r_{\mathrm{eff}},\theta,\tilde{z},\tilde{t}) = \frac{\partial \tilde{B}}{\partial \tilde{t}}. \tag{2.5a}$$

The introduction of the new unknown $\tilde{B}$ requires the imposition of another boundary condition, the mass action law, which states that the change in the bound state must be given by a Malthusian dissociation term, as well as a bimolecular production term:

$$\frac{\partial \tilde{B}}{\partial \tilde{t}} = \tilde{k}_{\mathrm{a}}\left[(B_{\mathrm{T}} - \tilde{B})\tilde{C}(r_{\mathrm{eff}}, \theta, \tilde{z}, \tilde{t}) - \tilde{K}\tilde{B}\right], \qquad \tilde{K} = \frac{\tilde{k}_{\mathrm{d}}}{\tilde{k}_{\mathrm{a}}}, \tag{2.5b}$$

where both of (2.5) hold only on the reacting strip. Here $\tilde{k}_{\mathrm{a}}$ and $\tilde{k}_{\mathrm{d}}$ are the rate constants, B_{T} is the total concentration of receptor sites, and $\tilde{K}$ is the equilibrium constant. In addition, we need an initial condition for $\tilde{B}$, which we take to be uniform on the reacting strip:

$$\tilde{B}(\theta, \tilde{z}, 0) = B_{\mathrm{T}} B_{\mathrm{i}}. \tag{2.6}$$

Here B_{i} represents the fraction of the receptor sites that are initially bound.

To reduce the problem to dimensionless variables, we normalize $\tilde{r}$ by the effective radius r_{eff} and time by the diffusion time scale, which will be shown to be the fastest. Note that due to the uniformity of our initial and boundary conditions, the only θ- and $\tilde{z}$-dependence in the problem enters through the helical reacting strip. Therefore, motivated by the form of (2.4), we switch to *helical coordinates* that are fixed in the reference frame of the reacting strip. Thus, we have the following scalings:

$$r = \frac{\tilde{r}}{r_{\mathrm{eff}}}, \qquad t_D = \frac{\tilde{t}D}{r_{\mathrm{eff}}^2}, \qquad y = \theta - \frac{\tilde{z}}{L}, \tag{2.7a}$$

$$C_D(r, y, t_D) = \frac{\tilde{C}(\tilde{r}, \theta, \tilde{z}, \tilde{t})}{C_{\mathrm{T}}}, \qquad B_D(y, t_D) = \frac{\tilde{B}(\theta, \tilde{z}, \tilde{t})}{B_{\mathrm{T}}}, \tag{2.7b}$$

where the D subscript indicates that we are normalizing by the diffusive time scale. Substituting (2.7) into (2.1)–(2.3) and (2.5), we have

$$\frac{\partial C_D}{\partial t_D} = \frac{1}{r}\frac{\partial}{\partial r}\left(r\frac{\partial C_D}{\partial r}\right) + \left(\frac{1}{r^2} + \lambda^2\right)\frac{\partial^2 C_D}{\partial y^2}, \qquad r \in [1, R], \quad y \in [0, 2\pi]; \qquad \lambda = \frac{r_{\mathrm{eff}}}{L}, \tag{2.8}$$

$$C_D(r, y, 0) = 1, \tag{2.9}$$

$$\frac{\partial C_D}{\partial r}(R, y, t_D) = 0, \tag{2.10a}$$

$$C_D(R, y, t_D) = 1, \tag{2.10b}$$

$$H(w - y)\frac{\partial B_D}{\partial t_D} = \gamma \frac{\partial C_D}{\partial r}(1, y, t_D), \tag{2.11a}$$

$$\gamma \equiv \frac{C_{\mathrm{T}} r_{\mathrm{eff}}}{B_{\mathrm{T}}} \approx \frac{\text{analyte available for binding}}{\text{binding sites}}, \tag{2.11b}$$

$$\frac{\partial B_D}{\partial t_D} = k_{\mathrm{a}}\left[(1 - B_D)C_D(1, y, t_D) - KB_D\right]H(w - y), \tag{2.12a}$$

$$k_{\mathrm{a}} = \frac{\tilde{k}_{\mathrm{a}} C_{\mathrm{T}} r_{\mathrm{eff}}^2}{D}, \qquad K = \frac{\tilde{K}}{C_{\mathrm{T}}}, \tag{2.12b}$$

where $H(w-y)$ is the Heaviside function that restricts (2.11a) and (2.12a) to the reacting strip. Here K is a dimensionless form of the equilibrium constant for the system and k_{a} is the "natural" dimensionless reaction rate (defined so that the forward reaction takes place on the time scale k_{a}^{-1}).

Combining (2.11a) and (2.12a), we have the following:

$$\frac{\partial C_D}{\partial r}(1,y,t_D) = \mathrm{Da}\left[(1-B_D)C_D(1,y,t_D) - KB_D\right]H(w-y), \tag{2.13a}$$

$$\mathrm{Da} \equiv \frac{k_{\mathrm{a}}}{\gamma} = \frac{\tilde{k}_{\mathrm{a}}B_{\mathrm{T}}}{D/r_{\mathrm{eff}}} = \frac{\text{reaction "velocity"}}{\text{diffusion "velocity"}}, \tag{2.13b}$$

where Da is the *Damköhler number* for the system. Lastly, we substitute (2.7) into (2.6) to obtain

$$B_D(y,0) = B_{\mathrm{i}}H(w-y). \tag{2.14}$$

3. General remarks.

3.1. Cases. Depending on the sizes of Da and γ, our work can fall into several cases. There are three time scales for this problem. The flow in the outer compartment equilibrates on the diffusion time scale. Another time scale, suggested by (2.11a), is the one characterizing diffusion into the reacting surface, which is γ^{-1} longer than the diffusive scale. The last time scale, suggested by (2.13a), is the time scale for the reaction, which is k_{a}^{-1} longer than the diffusive scale. The bound state evolves on the longer of these two time scales. If $\gamma = O(1)$, then the first two time scales are of the same order.

If $\mathrm{Da} = O(1)$, then the latter two time scales are of the same order. This case, where transport near the reacting surface balances the reaction, occurs often in CVD processes [6] and in rate constant measurement devices [19], [23].

To determine the proper scalings for our variables, we examine the material parameters, which are listed in Table 1. The value of r_{c} is calculated from the diameter of the DNA helix given in [3]. We use a large value for r_{eff} in order to ensure that our results will also model the case where larger molecules are binding to the helix. (It will be seen that the size of this parameter will not affect the underlying structure of the problem.) The period of the phosphate backbone rotation, $2\pi L$, is called the *helix pitch*. The value in the table is that of textbook B-form DNA [3]. The diffusivities listed are those for fibrinogen [21], peptides, and proteins [35].

We note that $\gamma \ll 1$, so to leading order (2.11a) becomes

$$\frac{\partial B_D}{\partial t_D} = 0 \qquad \Longrightarrow \qquad B_D(y,t_D) \equiv B_{\mathrm{i}}H(w-y), \tag{3.1}$$

where we have used (2.14). Hence, (2.13a) may be replaced by the following expression:

$$\frac{\partial C_D}{\partial r}(1,y,t_D) = \mathrm{Da}H(w-y)\left[(1-B_{\mathrm{i}})C_D(1,y,t_D) - KB_{\mathrm{i}}\right]. \tag{3.2}$$

Thus, in order to track the evolution of the bound state, we must introduce another time scale, which is the the one for the reaction. The proper scaling depends on the size of the Damköhler number [19], which Table 1 indicates is much smaller than 1 for the particular physical system at hand.

TABLE 1
Typical values of material parameters.

Parameter	Lower bound	Upper bound	Value used
B_{T} (mol/cm^2)	2.5×10^{-13} [35]	4×10^{-12} [35]	
C_{T} (mol/cm^3)	2.5×10^{-12} [35]	4×10^{-10} [35]	
D (cm^2/s)	2.8×10^{-7} [21]	10^{-6} [35]	
$\tilde{k}_{\mathrm{a}}$ (cm^3/mol $\cdot$ s)	6.5×10^{5} [36]	10^{10} [24]	
L (cm)			5.41×10^{-8} [3]
r_{a} (cm)	4.8×10^{-8} [27]	2.19×10^{-7} (NDB [29])	
r_{c} (cm)			10^{-7} [3]
r_{eff} (cm)	1.48×10^{-7}	3.19×10^{-7}	5×10^{-7}
Da	1.62×10^{-8}	1.43×10^{-2}	0.02
γ	6.25×10^{-8}	1.6×10^{-4}	
λ			9.24

We note that in this case (3.2) becomes

$$\frac{\partial C_D}{\partial r}(1, y, t_D) = 0. \tag{3.3}$$

Since the evolution of the bound state occurs on a slower time scale than t_D, we introduce the variables

$$t = k_{\mathrm{a}} t_D = \tilde{k}_{\mathrm{a}} C_{\mathrm{T}} \tilde{t}, \qquad C_D(r, y, t_D) = C(r, y, t) + o(1), \qquad B_D(y, t_D) = B(y, t) + o(1). \tag{3.4}$$

Note that t is the time scale on which the forward reaction occurs.

Substituting (3.4) into (2.8), (2.10), (2.11a), (2.12a), and (2.14), we have the following, to leading order:

$$\frac{1}{r}\frac{\partial}{\partial r}\left(r\frac{\partial C}{\partial r}\right) + \left(\frac{1}{r^2} + \lambda^2\right)\frac{\partial^2 C}{\partial y^2} = 0, \tag{3.5}$$

$$\frac{\partial C}{\partial r}(R, y, t) = 0, \tag{3.6a}$$

$$C(R, y, t) = 1, \tag{3.6b}$$

$$\frac{\partial C}{\partial r}(1, y, t) = H(w - y)\mathrm{Da}\frac{\partial B}{\partial t}, \tag{3.7}$$

$$\frac{\partial B}{\partial t} = [(1 - B)C(1, y, t) - KB]H(w - y), \tag{3.8}$$

$$B(y, 0) = B_{\mathrm{i}} H(w - y). \tag{3.9}$$

Clearly solutions of (3.5) are steady states of (2.8).

Note that our solutions will depend on the parameters k_{a} (through t) and K. Therefore, by taking measurements of B and comparing the results with our solutions, we can estimate K and k_{a}. Since C_{T} is known for each experiment, one can then easily estimate $\tilde{k}_{\mathrm{a}}$ and $\tilde{k}_{\mathrm{d}}$.

3.2. Steady state. Some useful information may be gleaned by examining the steady states of (2.8), (2.10b), and (2.11a), which we indicate by the subscript "s". It is clear that the steady-state solution in this case is $C_{\rm s}(r,y)\equiv 1$, and hence

$$B_{\rm s}(y)=\frac{H(w-y)}{\alpha},\qquad \alpha\equiv 1+K. \tag{3.10}$$

Thus K determines the final bound concentration. Noting the relationship between K and $C_{\rm T}$ in (2.12b), we see that by running several experiments with varying values of $C_{\rm T}$ and graphing $B_{\rm s}$ vs. $C_{\rm T}$, one can obtain an estimate for $\tilde{K}$. However, in order to get an appropriate estimate for both $\tilde{k}_{\rm a}$ and $\tilde{k}_{\rm d}$, we must have another piece of information, which we shall derive in later sections.

3.3. General structure. In order to examine the general underlying structure of this problem, we note that (3.5)–(3.8) are really a special case of the following problem, posed in an arbitrary spatial domain $\mathcal{R}$:

$$\mathcal{L}C=0,\quad \mathbf{x}\in\mathcal{R};\qquad \mathcal{F}C=0,\quad \mathbf{x}\in\partial\mathcal{R}_{\rm n};\qquad {\rm Da}\frac{\partial B}{\partial t}=\frac{\partial C}{\partial n},\quad \mathbf{x}\in\partial\mathcal{R}_{\rm r}; \tag{3.11}$$

$$\frac{\partial B}{\partial t}=(1-B)C-KB,\quad \mathbf{x}\in\partial\mathcal{R}_{\rm r}; \tag{3.12}$$

where $\partial/\partial n$ refers to the normal derivative, $\mathcal{L}$ is a linear operator, and $\mathcal{F}$ is an affine operator (both assumed to be independent of Da). Here $\partial\mathcal{R}_{\rm n}$ is the nonreacting boundary (in our system, $r=1$, $w<y<2\pi$, and $r=R$) and $\partial\mathcal{R}_{\rm r}$ is the reacting boundary (in our system, $r=1$, $0\le y\le w$).

Since we have assumed that $\gamma\ll 1$, $k_{\rm a}\ll{\rm Da}$, and thus we expand our dependent variables as series in Da:

$$C(\mathbf{x},t)=C_0(\mathbf{x},t)+{\rm Da}C_1(\mathbf{x},t)+o({\rm Da}), \tag{3.13a}$$

$$B(\mathbf{x},t)=B_0(\mathbf{x},t)+{\rm Da}B_1(\mathbf{x},t)+o({\rm Da}). \tag{3.13b}$$

Substituting (3.13) into (3.11) and (3.12), we obtain

$$\mathcal{L}C_0=0,\quad \mathbf{x}\in\mathcal{R};\quad \mathcal{F}_0C_0=0,\quad \mathbf{x}\in\partial\mathcal{R}_{\rm n};\quad \frac{\partial C_0}{\partial n}=0,\quad \mathbf{x}\in\partial\mathcal{R}_{\rm r}; \tag{3.14a}$$

$$\mathcal{L}C_1=0,\quad \mathbf{x}\in\mathcal{R};\quad \mathcal{F}_1C_1=0,\quad \mathbf{x}\in\partial\mathcal{R}_{\rm n};\quad \frac{\partial C_1}{\partial n}=\frac{\partial B_0}{\partial t},\quad \mathbf{x}\in\partial\mathcal{R}_{\rm r}; \tag{3.14b}$$

$$\frac{\partial B}{\partial t}=(1-B)(C_0+{\rm Da}C_1)-KB+O({\rm Da}^2),\quad \mathbf{x}\in\partial\mathcal{R}_{\rm r}; \tag{3.15}$$

where $\mathcal{F}C\sim\mathcal{F}_0C_0+{\rm Da}\mathcal{F}_1C_1$. Since $\mathcal{F}$ is affine and independent of Da, $\mathcal{F}_1$ must be linear.

If the solution C_0 of (3.14a) and the initial condition for B_0 are constant along $\partial\mathcal{R}_{\rm r}$ (which will be shown to be true in our cylindrical system), then the solution to the leading order of (3.15),

$$\frac{\partial B_0}{\partial t}=(1-B_0)C_0-KB_0,\quad \mathbf{x}\in\partial\mathcal{R}_{\rm r}, \tag{3.16}$$

is a function of time only. Since both $\mathcal{L}$ and $\mathcal{F}_1$ are linear, we may write

$$C_1=\frac{dB_0}{dt}h, \tag{3.17}$$

where h satisfies the first two equations in (3.14b) and

$$\frac{\partial h}{\partial n} = 1, \quad \mathbf{x} \in \partial\mathcal{R}_{\mathrm{r}}.$$

We note that the equations governing h do not involve the binding process, and hence h is a function of the geometry of the domain $\mathcal{R}$ and the transport process only.

In the next sections we calculate the solution in the case of both the Dirichlet condition (3.6b) and the Neumann condition (3.6a).

4. Dirichlet condition. Substituting (3.13) into (3.5) and (3.6b)–(3.9), we have, to leading two orders,

(4.1)
$$\frac{1}{r}\frac{\partial}{\partial r}\left(r\frac{\partial C_0}{\partial r}\right) + \left(\frac{1}{r^2} + \lambda^2\right)\frac{\partial^2 C_0}{\partial y^2} = 0, \qquad C_0(R, y, t) = 1, \qquad \frac{\partial C_0}{\partial r}(1, y, t) = 0,$$

$$\frac{\partial B_0}{\partial t} = [(1 - B_0)C_0(1, y, t) - KB_0]H(w - y), \tag{4.2a}$$

$$B_0(y, 0) = B_{\mathrm{i}}H(w - y), \tag{4.2b}$$

$$\frac{1}{r}\frac{\partial}{\partial r}\left(r\frac{\partial C_1}{\partial r}\right) + \left(\frac{1}{r^2} + \lambda^2\right)\frac{\partial^2 C_1}{\partial y^2} = 0, \qquad C_1(R, y, t) = 0, \tag{4.3a}$$

$$\frac{\partial C_1}{\partial r}(1, y, t) = \frac{\partial B_0}{\partial t}, \tag{4.3b}$$

$$\frac{\partial B_1}{\partial t} = H(w - y)[(1 - B_0)C_1(1, y, t) - B_1C_0(1, y, t) - KB_1], \tag{4.4a}$$

$$B_1(y, 0) = 0. \tag{4.4b}$$

Since the solution of the operator in (4.1) is a steady state of the operator in (2.8), we may use our steady-state discussion in section 3.2 to conclude that the solution of (4.1) is $C_0(r, y, t) \equiv 1$, and thus we obtain the evolution equation

$$\frac{\partial B_0}{\partial t} = (1 - \alpha B_0)H(w - y). \tag{4.5}$$

A brief discussion of (4.5) is appropriate. Rewriting the equation with the parameters and independent variables in dimensional form, we have the following:

$$\frac{\partial B_0}{\partial \tilde{t}} = \left[\tilde{k}_{\mathrm{a}}C_{\mathrm{T}} - \left(\tilde{k}_{\mathrm{a}}C_{\mathrm{T}} + \tilde{k}_{\mathrm{d}}\right)B_0\right]H(w - y), \tag{4.6}$$

where we have used (3.10), (3.4), (2.12b), and (2.5b). Therefore, in this case a plot of $\partial B_0/\partial\tilde{t}$ vs. B_0 at any point y will yield a straight line with slope

$$S = \tilde{k}_{\mathrm{a}}C_{\mathrm{T}} + \tilde{k}_{\mathrm{d}}. \tag{4.7}$$

Since C_{T} is a known quantity that can be varied from experiment to experiment, a graph of S *vs.* C_{T} will be a straight line with slope $\tilde{k}_{\mathrm{a}}$ and intercept $\tilde{k}_{\mathrm{d}}$. Note also that due to the special form of (4.7), we do not use the steady-state solution to provide information about K.

Solving (4.5) subject to (4.2b), we obtain

$$B_0(y,t) = \left(\frac{1-e^{-\alpha t}}{\alpha} + B_{\mathrm{i}} e^{-\alpha t}\right) H(w-y). \tag{4.8}$$

Of course, this is the standard type of exponential behavior one would expect from an operator like (4.5). In addition, we note that on the reacting strip B_0 is constant in y, as postulated in section 3.3, since both C_0 and B_{i} are constant in y. Therefore, noting that

$$\frac{\partial B_0}{\partial t} = \chi e^{-\alpha t} H(w-y), \qquad \chi = 1 - \alpha B_{\mathrm{i}}, \tag{4.9}$$

we obtain the substitution

$$C_1(r,y,t) = \chi e^{-\alpha t} h(r,y), \tag{4.10a}$$

where $h(r,y)$ satisfies (4.3a) and

$$\frac{\partial h}{\partial r}(1,y) = H(w-y). \tag{4.10b}$$

To solve for h, we introduce the standard notion of a complex Fourier series in the y-direction:

$$f(y) = \sum_{n=-\infty}^{\infty} f_n e^{iny}, \qquad f_n = \frac{1}{2\pi}\int_0^{2\pi} f(y) e^{-iny}\, dy.$$

In order to simplify our algebra, we write

$$h_n(r) = g_n(r)[H(w-y)]_n, \tag{4.11a}$$

where $[H(w-y)]_n$ is the finite Fourier transform of the Heaviside function and $g_n(r)$ satisfies

$$r^2 \frac{d^2 g_n}{dr^2} + r\frac{dg_n}{dr} - n^2(\lambda^2 r^2 + 1) g_n = 0, \qquad g_n(R) = 0, \qquad \frac{dg_n}{dr}(1) = 1. \tag{4.11b}$$

Equation (4.11b) is the modified Bessel equation of order n with respect to the parameter λr. Thus our solution is

$$g_n(r) = \begin{cases} \dfrac{I_n(\lambda n r) K_n(\lambda n R) - K_n(\lambda n r) I_n(\lambda n R)}{\lambda n [I_n'(\lambda n) K_n(\lambda n R) - K_n'(\lambda n) I_n(\lambda n R)]}, & n \neq 0, \\ \log\left(\dfrac{r}{R}\right), & n = 0. \end{cases} \tag{4.12}$$

We note from the operator in (4.11b) that $g_n(r)$ is even in n. The surface of interest is $r = 1$, where we have

$$C_1(1,y,t) = \chi e^{-\alpha t} h(1,y), \tag{4.13a}$$

$$h(1,y) = -\frac{w \log R}{2\pi} + \frac{1}{2i\pi} \sum_{\substack{n \in \mathcal{Z} \\ n \neq 0}} \frac{g_n(1) e^{iny}(1 - e^{-inw})}{n}. \tag{4.13b}$$

Substituting our expression for C_0, (4.8), and (4.13a) into (4.4a) and then solving yield

$$B_1(y,t) = \frac{\chi e^{-\alpha t} h(1,y)}{\alpha}\left[Kt - \frac{\chi}{\alpha}(e^{-\alpha t} - 1)\right], \tag{4.14}$$

where we have used (4.4b). Note that (4.14) is a secular term since for times larger than $O(\mathrm{Da}^{-1})$, it will be larger than the deviation of B_0 from the steady state B_s. However, this need not concern us, as any experiment can provide useful data on much shorter time scales.

5. Averaged expressions. Though from a mathematical point of view it may be nice to have closed-form expressions for C and B as functions of x and t, often from an experimental point of view the spatial average of B is of primary interest.

5.1. General structure. We begin by considering the general problem of section 3.3. Substituting (3.17) into (3.15) and rearranging, we have

$$\frac{\partial B}{\partial t} - \mathrm{Da}(1 - B_0)\frac{dB_0}{dt}h = (1 - B)C_0 - KB + O(\mathrm{Da}^2), \quad \mathbf{x} \in \partial\mathcal{R}_r. \tag{5.1}$$

We define the average of B in the usual way:

$$\bar{B}(t) = \frac{1}{|\partial\mathcal{R}_r|}\int_{\partial\mathcal{R}_r} B(\mathbf{x},t)\, dA,$$

where $|\partial\mathcal{R}_r|$ is the area of $\partial\mathcal{R}_r$. Performing this averaging procedure on (5.1), we obtain

$$\frac{d\bar{B}}{dt} = \frac{(1 - \bar{B})C_0 - K\bar{B}}{1 - \mathrm{Da}(1 - \bar{B})\bar{h}} + O(\mathrm{Da}^2), \quad \mathbf{x} \in \partial\mathcal{R}_r. \tag{5.2}$$

In the absence of transport, we have that $\mathrm{Da} = 0$, and (5.2) reduces to the standard ODE governing the reaction. However, if there is transport, the Da term describes the effect on the evolution of the bound state caused by the fact that the analyte is not in equilibrium. Since $\bar{h} < 0$, the $\mathrm{Da}\bar{h}$ term indicates the deficit in the supply of analyte due to imperfect transport. The $1 - \bar{B}$ term is the average concentration of vacant receptor sites available for rebinding.

Since we are studying a bimolecular reaction, the product of the terms is related to a binding probability. If we rewrite (5.2), we note that it is related to the *transport reduction* P in the probability of binding from the perfect binding case where the probability is 1:

$$\frac{d\bar{B}}{dt} = [(1 - \bar{B})C_0 - K\bar{B}](1 - P) + O(\mathrm{Da}^2), \qquad P = -\frac{\mathrm{Da}(1 - \bar{B})\bar{h}}{1 - \mathrm{Da}(1 - \bar{B})\bar{h}}. \tag{5.3}$$

Here P roughly represents the probability that a ligand available for binding will be swept away from a receptor site rather than bind to it. Thus using the standard ODE model when transport is important causes one to underestimate the true rate constant. However, using the effective rate constant model in (5.2) produces more correct estimates.

Therefore, if one wishes to obtain an effective rate constant equation as in (5.2), one need calculate only $\bar{h}$ if all the other assumptions in this section are satisfied. This usually occurs in biological systems of this type.

5.2. Cylindrical problem. In the cylindrical problem at hand, we note that the salient average is the one measured across the reacting strip:

$$\bar{B}(t) = \frac{1}{w}\int_0^w B(y,t)\,dy. \tag{5.4}$$

Taking the average of (4.8), we have

$$\bar{B}_0(t) = \frac{1-e^{-\alpha t}}{\alpha} + B_{\mathrm{i}}e^{-\alpha t}. \tag{5.5}$$

Averaging (4.14), we obtain the following:

$$\bar{B}_1(t) = \frac{\chi e^{-\alpha t}\bar{h}(1)}{\alpha}\left[Kt - \frac{\chi}{\alpha}(e^{-\alpha t}-1)\right]. \tag{5.6}$$

We also note that upon substituting $C_0 = 1$ into (5.2), we find that

$$\frac{d\bar{B}}{dt} = \frac{1-\alpha\bar{B}}{1-\mathrm{Da}(1-\bar{B})\bar{h}(1)} + O(\mathrm{Da}^2). \tag{5.7}$$

Evaluating $\bar{h}(1)$ while using the fact that g_n is even in n, we obtain

$$\bar{h}(1) = -\frac{w\log R}{2\pi} + \frac{2}{\pi w}\sum_{n=1}^{\infty}\frac{g_n(1)(1-\cos nw)}{n^2}. \tag{5.8}$$

Note that the terms in the sum decay like n^{-3} since g_n decays like n^{-1}.

Graphs of these results are shown in Figure 6.1.

6. Multiple-scale expansion for the Neumann condition. At the outer surface of the second compartment ($r = R$) we now impose the Neumann condition given by (2.10a) instead of the Dirichlet condition given by (2.10b). In this case, the boundary conditions at $r = R$ in (4.1) and (4.3a) are replaced by

$$\frac{\partial C_0}{\partial r}(R,y,t) = 0, \tag{6.1a}$$

$$\frac{\partial C_1}{\partial r}(R,y,t) = 0. \tag{6.1b}$$

We note that the solution to (4.1) (with the Dirichlet condition removed) and (6.1a) is an unknown constant. To determine it, we must return to the evolution on the t_D time scale. Since the reaction has not yet started, it is clear that the initial data has not been affected to leading order, and hence $C_0 \equiv 1$ is still the solution.

Therefore our expressions in (4.5) and (4.8) still hold, and so (4.11b) holds with the following new condition at $r = R$:

$$\frac{dg_n}{dr}(R) = 0. \tag{6.2}$$

Thus the solution is

$$g_n(r) = \frac{I_n(\lambda nr)K_n'(\lambda nR) - K_n(\lambda nr)I_n'(\lambda nR)}{\lambda n[I_n'(\lambda n)K_n'(\lambda nR) - K_n'(\lambda n)I_n'(\lambda nR)]}, \quad n \neq 0. \tag{6.3}$$

However, the case $n = 0$ is much more troublesome, for then (4.11b) becomes

$$r^2 \frac{d^2 g_0}{dr^2} + r \frac{dg_0}{dr} = 0, \qquad \frac{dg_0}{dr}(R) = 0, \qquad \frac{dg_0}{dr}(1) = 1.$$

Since the condition at $r = R$ is fixed, this equation has no solution unless dg_0/dr is really zero, which can occur only if the rate of change of the mean of the bound state ($dB_{,0}/dt$) is zero; but this is not true, and hence we have a contradiction. This results from the fact that we are trying to solve Laplace's equation with no flux through one boundary and a nonzero flux at the other.

To resolve this paradox, we note that the full problem actually has a time derivative that can compensate for the nonzero flux. The trouble occurs because we have separated the two time scales t and t_D in our perturbation analysis. Hence we must use both scales in our solution for C. Since the problem appears at first order and only in the zeroth mode, we now let

$$C_D(r, y, t_D) = 1 + \mathrm{Da} \sum_{n=-\infty}^{\infty} c_n(r, t_D, t) e^{iny} \tag{6.4}$$

and focus on c_0. At the present stage we consider this to be an *exact* transformation; we shall consider a perturbation series later. (We do not adjust our form for B. Doing so would simply lead to $\partial B/\partial t_D = 0$ as in section 3.1.) Substituting (6.4) and our form for B into (2.8), (2.9), (2.10a), and (2.11a), we have, to leading order,

(6.5a)
$$\frac{1}{r}\frac{\partial}{\partial r}\left(r \frac{\partial c_0}{\partial r}\right) = \frac{\partial c_0}{\partial t_D} + k_\mathrm{a} \frac{\partial c_0}{\partial t}, \qquad \frac{\partial c_0}{\partial r}(1, t_D, t) = \frac{dB_{,0}}{dt}, \qquad \frac{\partial c_0}{\partial r}(R, t_D, t) = 0,$$

$$c_0(r, 0, 0) = 0, \tag{6.5b}$$

where we denote the nth Fourier coefficient of B by $B_{,n}$.

Equations (6.5) allow a separation-of-variables solution of the following form:

(6.6a)
$$c_0(r, t_D, t) = \sum_{m=1}^{\infty} a_{,m}(t_D, t)\phi_m(r), \qquad a_{,m}(t_D, t) = \frac{1}{p_m} \int_1^R r\phi_m(r) c_0(r, t_D, t)\, dr,$$

$$p_m = \int_1^R r\phi_m^2\, dr, \tag{6.6b}$$

where $\phi_m(r)$ satisfies the homogeneous system

$$\frac{d^2\phi_m}{dr^2} + r\frac{d\phi_m}{dr} + \nu_m^2 r^2 \phi_m = 0, \qquad \phi_m'(1) = \phi_m'(R) = 0, \qquad \nu_m > 0. \tag{6.7}$$

Since this is an eigenvalue problem, we may pick an additional normalization. We choose to set $\phi_m(1) = 1$. Then the solution of (6.7) is

$$\phi_m(r) = \frac{Y_1(\nu_m R)J_0(\nu_m r) - J_1(\nu_m R)Y_0(\nu_m r)}{Y_1(\nu_m R)J_0(\nu_m) - J_1(\nu_m R)Y_0(\nu_m)}, \tag{6.8a}$$

$$Y_1(\nu_m R)J_1(\nu_m) = J_1(\nu_m R)Y_1(\nu_m). \tag{6.8b}$$

Multiplying the operator in (6.5a) by $r\phi_m$ and integrating from $r = 1$ to $r = R$ while using the boundary conditions in (6.5a), we have

$$-\frac{1}{p_m}\frac{dB_{,0}}{dt} - \nu_m^2 a_{,m} = \frac{\partial a_{,m}}{\partial t_D} + k_{\mathrm{a}}\frac{\partial a_{,m}}{\partial t}. \tag{6.9a}$$

The initial condition for (6.9a) results from (6.5b):

$$a_{,m}(0,0) = 0. \tag{6.9b}$$

Since we have reduced the number of variables in the problem, we now exploit the smallness of k_{a} by assuming the following series expansion for $a_{,m}$ and $B_{,0}$:

$$a_{,m}(t_D, t; k_{\mathrm{a}}) \sim a_{0,m}(t_D, t) + k_{\mathrm{a}} a_{1,m}(t_D, t) + \cdots,$$

$$B_{,0}(t; k_{\mathrm{a}}) \sim B_{0,0}(t) + k_{\mathrm{a}} B_{1,0}(t) + \cdots.$$

Note that we are using the same subscript notation for a different series from the one in section 4. However, this does not matter since it is only the leading-order term with which we will be concerned, and this will be the same in both cases. Thus the first two orders of (6.9) become

$$-\frac{1}{p_m}\frac{dB_{0,0}}{dt} - \nu_m^2 a_{0,m} = \frac{\partial a_{0,m}}{\partial t_D}, \qquad a_{0,m}(0,0) = 0, \tag{6.10a}$$

$$-\frac{1}{p_m}\frac{dB_{1,0}}{dt} - \nu_m^2 a_{1,m} = \frac{\partial a_{1,m}}{\partial t_D} + \frac{\partial a_{0,m}}{\partial t}, \qquad a_{1,m}(0,0) = 0. \tag{6.10b}$$

The solution of (6.10a) is

$$a_{0,m}(t_D, t) = -\frac{1}{p_m \nu_m^2}\frac{dB_{0,0}}{dt} + f(t)\exp\left(-\nu_m^2 t_D\right), \qquad f(0) = \frac{1}{p_m\nu_m^2}\frac{dB_{0,0}}{dt}(0). \tag{6.11}$$

To calculate the right-hand side of the initial condition, we note that if we now consider Da to be small, we may use our previous expression for $\partial B_0/\partial t$ to obtain $B_{0,n}$, and hence

$$f(0) = \frac{w\chi}{2\pi p_m \nu_m^2}. \tag{6.12}$$

Substituting (6.11) into (6.10b) and rearranging, we obtain

$$\frac{\partial a_{1,m}}{\partial t_D} + \nu_m^2 a_{1,m} = -\frac{1}{p_m}\frac{dB_{1,0}}{dt} + \frac{1}{p_m\nu_m^2}\frac{d^2 B_{0,0}}{dt^2} - f'(t)\exp\left(-\nu_m^2 t_D\right). \tag{6.13}$$

Hence for there to be no forcing at resonance, $f(t)$ must be a constant. Therefore, our solution is given by the following:

$$a_{0,m}(t_D, t) = \frac{1}{p_m\nu_m^2}\left[\frac{w\chi}{2\pi}\exp\left(-\nu_m^2 t_D\right) - \frac{dB_{0,0}}{dt}\right]. \tag{6.14}$$

Note that we have essentially treated t as a parameter, and recalling the differing time scales, on the t time scale we have that

$$C_{1,0}(1,t) = \lim_{t_D\to\infty} c_{,0}(1,t,t_D) = -\sum_{m=1}^{\infty}\frac{1}{p_m\nu_m^2}\frac{dB_{,0}}{dt}. \tag{6.15}$$

TABLE 2
First several eigenvalues, $R = 4$.

m	p_m	ν_m	m	p_m	ν_m
1	1.899	1.112	6	1.517	6.298
2	1.633	2.134	7	1.513	7.343
3	1.565	3.170	8	1.510	8.389
4	1.538	4.210	9	1.508	9.435
5	1.525	5.253	10	1.506	10.481

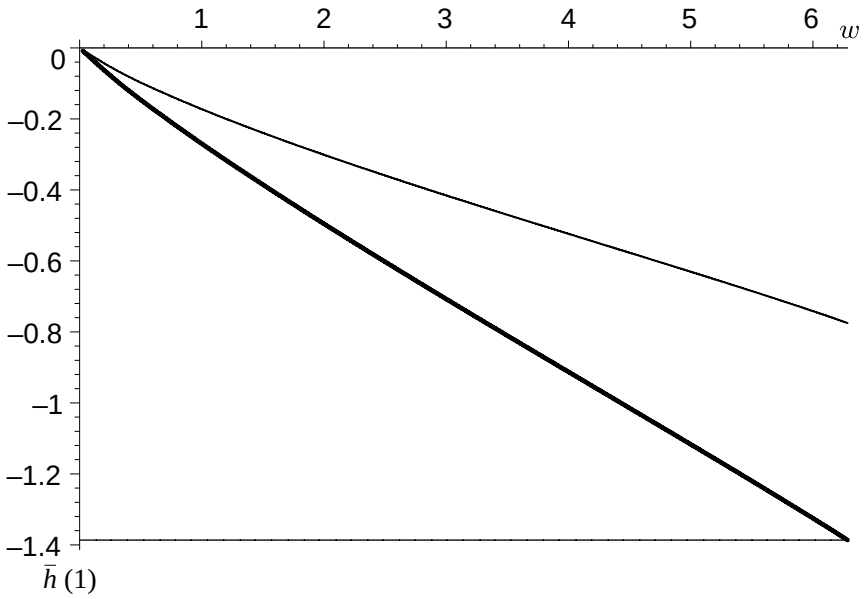

FIG. 6.1. *$\bar{h}(1)$ and $-\log R$ (thin line) vs. w for $\lambda = 9.24$, $R = 4$ (medium line: Neumann; thick line: Dirichlet).*

Using our new definition of $g_n(r)$ in (6.4), we see that (4.13b) now becomes the following:

$$h(1,y) = -\frac{w}{2\pi}\sum_{m=1}^{\infty}\frac{1}{p_m\nu_m^2} + \frac{1}{2i\pi}\sum_{\substack{n\in\mathcal{Z}\\ n\neq 0}}\frac{g_n(1)e^{iny}(1-e^{-inw})}{n}. \tag{6.16}$$

Note that the first sum is a function of R only.

The rest of the equations in section 4 still hold with our new definition of $h(y)$. Therefore, the only change to the results of section 5 is the replacement of the first term in (5.8) with the first sum in (6.16). To show how quickly the terms decay, in Table 2 we list the first 10 values of p_m and ν_m for $R = 4$. (This choice of R corresponds to a DNA volume fraction of roughly 0.25%.) We note that ν_m increases roughly linearly with m, and hence to get the same error in $\bar{h}(1)$ we must take more terms in the first sum (where the terms decay like m^{-2}) than in the second sum (where the terms decay like n^{-3}).

In Figure 6.1 we display a plot of $\bar{h}(1)$ vs. w for the Dirichlet problem, indicated by the thick line, using the first 10 terms of (5.8). The parameters used are $\lambda = 9.24$ and $R = 4$. If $w = 0$, there is no reacting strip, and hence there is no deviation from the equilibrium solution. Therefore in this case $\bar{h}(1) = 0$. If $w = 2\pi$, the

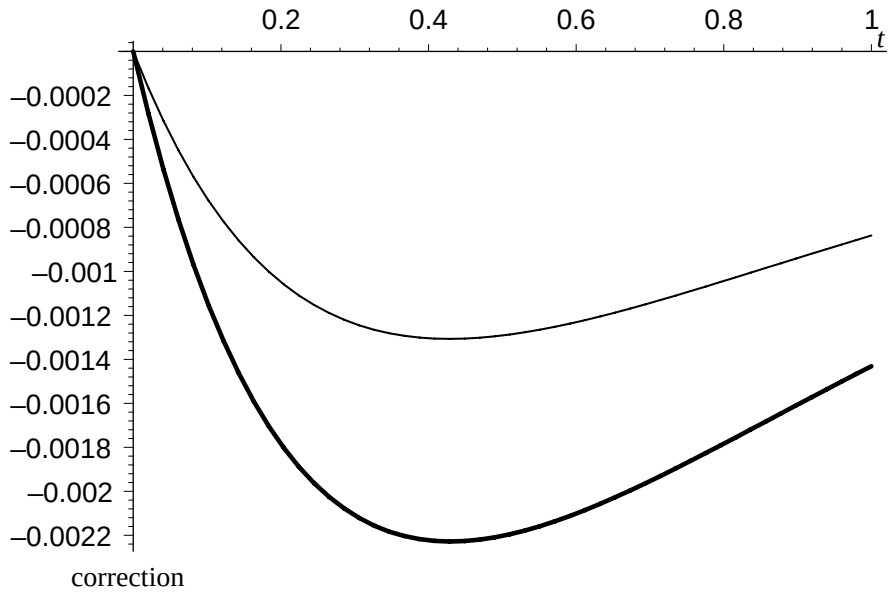

FIG. 6.2. *Effect of transport on* $\bar{B}(t)$ *from Dirichlet (thick) and Neumann (thin) lines,* $\lambda = 9.24$, $R = 4$, $w = \pi$, $\mathrm{Da} = 0.02$.

entire cylinder is reacting and the problem has no θ-dependence. Thus the infinite sum drops out and $\bar{h}(1) = -\log R$. As the width of the reacting strip increases, the analyte must diffuse to a larger area to keep the reaction going. Therefore, the net effect of transport upon the reaction increases with increasing w.

Figure 6.1 also shows a graph for the Neumann case, indicated by the medium line, which has been calculated by adding the first 32 terms of the first sum in (6.16). We note that the average value is lower in the Dirichlet case. In the Neumann case, the concentration at the outer boundary need not remain at $C = 1$. Therefore, as analyte binds to the surface, a steep concentration gradient need not form since no new analyte is entering the system. Combining (4.10), (4.11a), and (4.13a), we obtain

$$\frac{\partial C_{1,n}}{\partial r}(1,t) = -\frac{1}{g_n(1)} C_{1,n}(r,t).$$

Therefore, a smaller gradient implies a larger (less negative) value for $\bar{h}(1)$.

Figure 6.2 shows the corresponding deviation of the solution given by (5.7) from that in (5.5) for the two different boundary conditions for the case when $w = \pi$ and $\mathrm{Da} = 0.02$. Note that with a less negative value of $\bar{h}(1)$, the effects of transport are smaller in the Neumann case. Therefore, the Neumann solution is closer to the equilibrium solution.

This concludes our examination of association kinetics; the case of dissociation kinetics is discussed in the appendix.

7. Conclusions. Key to the understanding of certain biological reactions are the values of their association and dissociation rate constants. However, in order to translate experimental measurements into useful estimates of the rate constants, accurate mathematical models are needed.

We presented the full set of transport-reaction equations for the system. By making reasonable assumptions about the DNA geometry, we were able to transform our

equations into helical coordinates. The introduction of proper dimensionless variables demonstrated that in the case without bulk flow there are three separate time scales associated with the problem. On the diffusive time scale the concentration of unbound ligand in the channel equilibrates as if no receptors are present. Whenever diffusion into the binding surface dominates, the evolution of the bound state evolves on that time scale. However, in the more physically realizable case, the evolution of the bound state evolves on the reaction time scale t.

Scaling also showed that the key dimensionless group is the Damköhler number, Da, which measures the ratio of the time scales of reaction and diffusion. If $\mathrm{Da} \ll 1$, the reaction kinetics decouple from the transport effects and to leading order our model produces the well-known result from kinetic theory [17]. The form of the next-order correction for small Da depends on the quantity $\bar{h}$, which measures the average correction due to transport. The calculation of $\bar{h}$ in the case with Dirichlet condition was relatively straightforward.

In the Neumann case, in order to resolve the nonzero-flux paradox for the resulting Laplace's equation, a multiple-scale expansion was used. The way in which the secular terms appeared in the equations was highly unusual and clearly suggested the inappropriateness of considering the diffusion and reaction time scales separately.

Once the solutions were obtained, we constructed averages since they are what experimentalists measure in practice. Examination of these averages showed that the solution for the bound state to leading two orders in Da may be written as the solution of an ODE. The effective rate constants in this ODE demonstrated the effects of transport on the reaction. We showed that these effective rate constants appear in a wide class of problems associated with these systems.

In addition to providing improved estimates to the rate constants in selected situations, the careful modeling and scaling in sections 2 and 3 provides a sturdy mathematical framework for further studies in cylindrical geometries. In particular, further research will focus on the effect of external analyte flow on the reaction process.

We also note that the Dirichlet and Neumann conditions (2.3) considered in this work are simply special cases of the radiation condition

$$\tilde{D}\frac{\partial \tilde{C}}{\partial \tilde{r}}(r_{\mathrm{eff}}R, \theta, \tilde{z}, \tilde{t}) = \kappa(C_{\mathrm{T}} - \tilde{C}(r_{\mathrm{eff}}R, \theta, \tilde{z}, \tilde{t})), \tag{7.1}$$

where κ is a measure of the "permeability" of the outer boundary. Here the Dirichlet condition is the limit of (7.1) as $\kappa \to \infty$ and the Neumann condition is the limit of (7.1) as $\kappa \to 0$. Therefore, another interesting avenue of further research would be to examine the system for the full flux condition (7.1). In particular, we might expect the $\kappa = 0$ limit to be singular due to the nature of the new expansion needed. However, the small κ limit may lead to other interesting behavior, such as the influence of the correction term on the $O(1)$ solution, as in [37].

8. Nomenclature.

8.1. Variables and parameters. Units are listed in terms of length (L), moles (N), or time (T). If the same letter appears both with and without tildes, the letter with a tilde has dimensions, while the letter without a tilde is dimensionless. Boldface letters indicate vectors. The equation where a quantity first appears is listed, if appropriate.

$a(\cdot)$: amplitude function for eigenfunction expansion (6.6a).
$\tilde{B}(\theta, \tilde{z}, \tilde{t})$: bound ligand concentration on surface $\tilde{r} = r_{\text{eff}}$ at position $(\theta, \tilde{z})$ and time $\tilde{t}$, units N/L^2 (2.5a).
$\tilde{C}(\tilde{r}, \theta, \tilde{z}, \tilde{t})$: unbound ligand concentration at position $(\tilde{r}, \theta, \tilde{z})$ and time $\tilde{t}$, units N/L^3 (2.1).
$c_n(r, t_D, t)$: Fourier coefficient of unbound ligand concentration in multiple-scale expansion (6.4).
D: molecular diffusion coefficient, units L^2/T (2.1).
Da: the Damköhler number, which measures the ratio of reaction and diffusion effects, value k_{a}/γ.
$\mathcal{F}$: boundary operator in generalized problem (3.11).
$f(\cdot)$: arbitrary function, variously defined.
$g_n(r)$: eigenfunction, variously defined (4.11a).
$h(\cdot)$: analyte concentration for uniform boundary conditions (3.17).
$\tilde{K}$: equilibrium constant for system, defined as $\tilde{k}_{\text{d}}/\tilde{k}_{\text{a}}$, units N/L^3 (2.5b).
$\tilde{k}_{\text{a}}$: association rate constant, units $L^3/(NT)$.
$\tilde{k}_{\text{d}}$: dissociation rate constant, units T^{-1}.
$\mathcal{L}$: linear operator (3.11).
L: wavelength of helical structure, units L (2.1).
m: indexing variable.
n: normal direction (3.11) or indexing variable.
P: transport reduction in probability of binding (5.3).
p_m: normalization constant for eigenfunction ϕ_m (6.6a).
$\mathcal{R}$: region containing analyte in generalized problem (3.11).
R: dimensionless radius of external compartment.
$\tilde{r}$: variable in radial direction, units L.
S: slope of a line (4.7).
$\tilde{t}$: dimensional time, units T (2.1).
w: radian measure of the reacting strip.
$\mathbf{x}$: spatial variable in generalized problem (3.11).
y: variable that fixes the helical strip position, defined as $\theta - \tilde{z}/L$ (2.7a).
$\mathcal{Z}$: the integers.
$\tilde{z}$: variable along the cylindrical structure, units L (2.1).
α: dimensionless constant, defined as $1 + K$ (3.10).
γ: dimensionless constant, defined as $C_{\text{T}} r_{\text{eff}}/B_{\text{T}}$ (2.11a).
θ: angular coordinate (2.1).
κ: permeability constant, units L/T (7.1).
λ: aspect ratio of cylinder, defined as r_{eff}/L (2.8).
ν_m: positive square root of eigenvalue for Neumann problem (6.7).
$\phi_m(r)$: eigenfunction for Neumann problem (6.6a).
χ: dimensionless constant, defined as $1 - \alpha B_{\text{i}}$ (4.9).

8.2. Other notation.

a: as a subscript on r, used to indicate the analyte molecule.
c: as a subscript, used to indicate the cylinder.
D: as a subscript, used to indicate the diffusive time scale (2.7a).
eff: as a subscript, used to indicate the effective cylinder.
i: as a subscript, used to indicate the initial state of a quantity (2.6).

$n \in \mathcal{Z}$: as a subscript, used to indicate a term in an expansion in Da (3.13a) or eigenfunctions.
n: as a subscript, used to indicate the nonreacting portion of the boundary in the generalized problem (3.11).
r: as a subscript, used to indicate the reacting portion of the boundary in the generalized problem (3.11).
s: as a subscript, used to indicate the steady state.
T: as a subscript, used to indicate the total value of a quantity (2.2).
$\bar{\ }$: used to denote the mean of the bound concentration over the reacting surface.

Appendix. Dissociation. In the main body of this paper, we focused on association kinetics, where the primary mechanism is the binding of ligand and receptor. However, an equally important system involves dissociation kinetics, where there is no analyte and hence the bound state must dissociate to achieve equilibrium.

In a typical dissociation experiment, the environment surrounding the cylinder is evacuated of all analyte. Thus, initially we have

$$C_D(r, y, 0) = 0, \tag{A.1}$$

and at the boundary of the exterior compartment we have one of the following conditions:

$$C_D(R, y, t_D) = 0, \qquad \frac{\partial C_D}{\partial r}(R, y, t_D) = 0. \tag{A.2}$$

Due to the linear nature of the transport operator, we see that by letting

$$\text{(association) } C_D \mapsto 1 - C_D \text{ (dissociation)}, \tag{A.3}$$

we obtain a solution to the transport equation. The value of this new solution for the analyte at the reacting surface will then affect the evolution of the bound state there.

In particular, in this case we have $C_0 \equiv 0$, and hence (4.5) becomes

$$\frac{\partial B_0}{\partial t} = -K B_0 H(w - y), \tag{A.4}$$

and its dimensional counterpart (4.6) becomes the following:

$$\frac{\partial B_0}{\partial \tilde{t}} = -\tilde{k}_{\mathrm{d}} B_0 H(w - y).$$

Thus to leading order, no association kinetics occur, and hence a plot of $\partial B_0/\partial \tilde{t}$ vs. B_0 will yield a straight line with slope $S = -\tilde{k}_{\mathrm{d}}$.

A typical dissociation experiment occurs after the association phase has reached steady state; hence, our initial condition is given by (3.10):

$$B_0(y, 0) = \frac{H(w - y)}{\alpha}. \tag{A.5}$$

Solving (A.4) subject to (A.5), we obtain

$$B_0(y, t) = H(w - y)\frac{e^{-Kt}}{\alpha}. \tag{A.6}$$

Of course, this is the standard type of exponential behavior one would expect.

We begin by considering the case where the Dirichlet condition is given. Since the operators and boundary conditions are the same for C_1 in both cases, the analysis through (4.13a) holds, but (4.9) becomes

$$\frac{\partial B_0}{\partial t} = -\frac{Ke^{-Kt}}{\alpha} H(w-y). \tag{A.7}$$

Substituting (A.7) into (4.13a), we obtain

$$C_1(1,y,t) = -\frac{Ke^{-Kt}}{\alpha} h(1,y), \tag{A.8}$$

where $h(y)$ is as defined in (4.13b). Substituting (A.6) and (A.8) into (4.4a), we have the following:

$$B_1(y,t) = -\frac{e^{-Kt}h(1,y)}{\alpha}\left(Kt + \frac{e^{-Kt}-1}{\alpha}\right), \tag{A.9}$$

where we have used (4.4b). Note that we again have a secular term. Our averaged expression becomes

$$\frac{d\bar{B}}{dt} = \frac{-K\bar{B}}{1-\mathrm{Da}(1-\bar{B})\bar{h}(1)} + O(\mathrm{Da}^2), \tag{A.10}$$

which is exactly analogous to (5.7) except that to leading order there is no association.

If instead we use the Neumann condition, all the analysis in section 6 holds, except now (6.14) is replaced by

$$a_{0,m}(t_D,t) = -\frac{1}{p_m\nu_m^2}\left[\frac{wK}{2\pi\alpha}\exp\left(-\nu_m^2 t_D\right) + \frac{dB_{0,0}}{\partial t}\right], \tag{A.11}$$

and hence since C_1 is as given in (A.8), the new definition of $h(y)$ in (6.16) does not change.

Acknowledgments. The author wishes to thank Donald S. Cohen for helpful discussions regarding the mathematics in this paper and Byron Goldstein for his invaluable discussions regarding the biophysics in this paper. Many of the calculations herein were checked using Maple.

REFERENCES

[1] B. Goldstein and M. Dembo, *Approximating the effects of diffusion on reversible reactions at the cell surface: Ligand-receptor kinetics*, Biophys. J., 68 (1995), pp. 1222–1230.
[2] A. Szabo, L. Stolz, and R. Granzow, *Surface plasmon resonance and its use in biomolecular interaction analysis (BIA)*, Curr. Opin. Struct. Bio., 5 (1995), pp. 699–705.
[3] R. R. Sinden, *DNA Structure and Function*, Academic Press, San Diego, 1994.
[4] B. Alberts, D. Bray, J. Lewis, M. Raff, K. Roberts, and J. D. Watson, *Molecular Biology of the Cell*, 3rd ed., Garland Publishing, New York, 1994.
[5] R. B. Bird, W. E. Stewart, and E. N. Lightfoot, *Transport Phenomena*, Wiley, New York, 1960.
[6] Y. F. Wang and R. Pollard, *An approach for modeling surface-reaction kinetics in chemical vapor deposition processes*, J. Electrochem. Soc., 142 (1995), pp. 1712–1725.
[7] P. Duverneuil and J. P. Couderc, *Two-dimensional modeling of low-pressure chemical vapor deposition hot wall tubular reactors. 1. Hypotheses, methods, and first results*, J. Electrochem. Soc., 139 (1992), pp. 296–304.

[8] M. Michaelidis and R. Pollard, *Analysis of chemical vapor deposition of boron*, J. Electrochem. Soc., 131 (1984), pp. 860–868.
[9] K. F. Jensen, *Modeling of chemical vapor deposition reactors for the fabrication of microelectronic devices*, in Chemical and Catalytic Reactor Modeling, ACS, Washington, DC, 1984.
[10] G. Eigenberger, *Modelling and simulation in industrial chemical reaction engineering*, in Modelling of Chemical Reaction Systems, Springer-Verlag, Heidelberg, 1981.
[11] E. D. Rusu, *Mass transport with enzyme reactions*, Acta Mech., 127 (1998), pp. 183–191.
[12] T. Kobayashi and K. Laidler, *Theory of the kinetics of reactions catalyzed by enzymes attached to the interior surface of tubes*, Biotech. Bioeng., 16 (1974), pp. 99–118.
[13] D. Basmadjian, *The effect of flow and mass transport in thrombogenesis*, Ann. Biomed. Eng., 18 (1990), pp. 685–709.
[14] V. T. Turitto and H. R. Baumgartner, *Platelet deposition on subendothelium exposed to flowing blood: Mathematical analysis of physical parameters*, Transactions Amer. Soc. Artif. Int. Org., 21 (1975), pp. 593–601.
[15] D. Basmadjian and M. V. Sefton, *A model of thrombin inacativation in heparinized and non-heparinized tubes with consequences for thrombus formation*, J. Biomed. Mat. Res., 20 (1986), pp. 633–651.
[16] E. F. Grabowski, L. I. Friedman, and E. F. Leonard, *Effects of shear rate on the diffusion and adhesion of blood platelets to a foreign surface*, Ind. Eng. Chem. Fund., 11 (1972), pp. 224–232.
[17] D. J. O'Shannessy, *Determination of kinetic rate and equilibrium binding constants for macromolecular interactions: A critique of the surface plasmon resonance literature*, Curr. Opin. Biotech., 5 (1994), pp. 65–71.
[18] R. Karlsson, H. Roos, L. Fägerstam, and B. Persson, *Kinetic and concentration analysis using BIA technology*, Methods, 6 (1994), pp. 99–110.
[19] D. A. Edwards, *Estimating rate constants in a convection-diffusion system with a boundary reaction*, IMA J. Appl. Math., 63 (1999), pp. 89–112.
[20] R. Glaser, *Antigen-antibody binding and mass transport by convection and diffusion to a surface: a two-dimensional computer model of binding and dissociation kinetics*, Anal. Biochem., 213 (1993), pp. 152–161.
[21] B. K. Lok, Y.-L. Cheng, and C. R. Robertsa, *Protein adsorption on crosslinked polydimethylsiloxane using total internal reflection fluorescence*, J. Coll. Int. Sci., 91 (1983), pp. 104–116.
[22] T. Mason, A. R. Pineda, C. Wofsy, and B. Goldstein, *Effective rate models for the analysis of transport-dependent biosensor data*, Math. Biosci., 159 (1999), pp. 123–144.
[23] D. A. Edwards, B. Goldstein, and D. S. Cohen, *Transport effects on surface-volume biological reactions*, J. Math. Biol., 39 (1999), pp. 533–561.
[24] D. G. Myszka, *Kinetic analysis of macromolecular interactions using surface plasmon resonance biosensors*, Curr. Opin. Biotech., 8 (1997), pp. 50–57.
[25] D. G. Myszka, X. He, M. Dembo, T. A. Morton, and B. Goldstein, *Extending the range of rate constants available from BIAcore™: Interpreting mass transport influenced binding data*, Biophys. J., 75 (1998), pp. 583–594.
[26] D. A. Edwards, *An alternative example of the method of multiple scales*, SIAM Rev., to appear.
[27] J. A. Mountzouris and L. H. Hurley, *Small molecule-DNA interaction*, in Bioorganic Chemistry: Nucleic Acids, Oxford University Press, New York, 1996.
[28] R. L. P. Adams, R. H. Burdon, A. M. Campbell, and R. M. S. Smellie, *Davidson's The Biochemistry of Nucleic Acids*, 8th ed., Academic Press, New York, 1976, p. 91.
[29] H. M. Berman, W. K. Olson, D. L. Beveridge, J. Westbrook, A. Gelbin, T. Demeny, S.-H. Hsieh, A. R. Srinivasan, and B. Schneider, *The nucleic acid database: A comprehensive relational database of three-dimensional structures of nucleic acids*, Biophys. J., 63 (1992), pp. 751–759.
[30] M. Lee, A. L. Rhodes, M. D. Wyatt, S. Forrow, and J. A. Hartley, *GC-base sequence recognition by oligo(imidazolecarboxamide) and C-terminus-modified analogs of distamycin deduced from circular dichroism, proton nuclear magnetic resonance, and methidiumpropylethylenediaminetetraacetate-iron*(II) *footprinting studies*, Biochem., 32 (1993), pp. 4237–4245.
[31] S. E. Swalley, E. E. Baird, and P. B. Dervan, *Effects of gamma-turn and beta-tail amino acids on sequence-specific recognition of DNA by hairpin polyamides*, J. Am. Chem. Soc., 121 (1999), pp. 1113–1120.
[32] H. C. Berg and E. M. Purcell, *Physics of chemoreception*, Biophys. J., 20 (1977), pp. 193–

219.

[33] B. Goldstein, C. Wofsy, and H. Echavarría-Heras, *Effect of membrane flow on the capture of receptors by coated pits*, Biophys. J., 53 (1988), pp. 405–414.

[34] D. C. Torney and B. Goldstein, *Rates of diffusion-limited reaction in periodic systems*, J. Stat. Phys., 49 (1987), pp. 725–750.

[35] M. L. Yarmush, D. B. Patankar, and D. M. Yarmush, *An analysis of transport resistance in the operation of BIAcore*$^{\text{TM}}$*: Implications for kinetic studies of biospecific interactions*, Molec. Immun., 33 (1995), pp. 1203–1214.

[36] W. Chen, S. Khilko, J. Fecondo, D. H. Margulies, and J. McCluskey, *Determinant selection of major histocompatibility complex class* I*-restricted antigenic peptides is explained by class* I*-peptide affinity and is strongly influenced by nondominant anchor residues*, J. Exper. Med., 180 (1994), pp. 1471–1483.

[37] A. K. Kapila, *Asymptotic Treatment of Chemically Reacting Systems*, Pitman, Boston, 1983, p. 95.